

Estimating the risk of wildfires in the municipality of Rio Verde, Goiás State, Central Brazil

Estimativa do risco de incêndios florestais no município de Rio Verde (GO), Brasil

Lucas Soares da Silva Aires¹ , Lucas Peres Angelini¹ , Victor Hugo de Moraes Danelichen² 

ABSTRACT

The damage caused by wildfires has major impacts each year, not only on the environment but also on the economy and public health. The present study aimed at mapping the fire risk in the different areas of the municipality of Rio Verde, in the Central Brazilian state of Goiás. A number of factors that influence the occurrence of wildfires were considered in this analysis, including the orientation of the relief, the slope, population density, proximity of homes, the road network, and land cover and use. The analytical hierarchy process was used to determine the appropriate weights for each of the variables. The fire risk index was divided into five classes: water, low, moderate, high, and very high risks. Class 4 (high risk) was the most frequently recorded within the study area, followed by classes 3 (moderate risk) and 2 (low risk). Subsequently, the heat spots recorded by remote sensing were related to fire risk indices, and the framing in the classes was verified. Overall, 16.36% of the heat spots were considered low risk (class 2), while 36.29% were classified as moderate risk (class 3), and 46.72% as high risk (class 4). These findings indicate that the fire risk index provides an adequate and effective parameter for the spatial assessment of the distribution of fire events (controlled burns or wildfires) in the municipality of Rio Verde.

Keywords: wildfires; risk modeling; vegetation; remote sensing.

RESUMO

Os danos causados pelos florestais têm incêndios causam grandes impactos todos os anos, não só no meio ambiente, mas também na economia e na saúde pública. O presente trabalho objetivou mapear o risco de incêndio nas diferentes áreas do município de Rio Verde, em Goiás, Brasil. Vários fatores que influenciam a ocorrência de incêndios florestais como a orientação do relevo, declividade, densidade populacional, proximidade das residências, rede de estradas e a cobertura e uso do solo, foram considerados na análise. Os pesos apropriados das variáveis foram designados usando o método de processo hierárquico analítico. O índice de risco de incêndio foi dividido em cinco classes: água, grau baixo, moderado, alto e muito alto. A classe 4 (risco alto) foi a mais frequente registrada dentro da área de estudo, seguida das classes 3 (risco moderado) e 2 (risco baixo). Posteriormente, os focos de calor registrados por sensoriamento remoto foram relacionados aos índices de risco de incêndio e verificado o enquadramento nas classes. No geral, 16,36% dos focos de calor foram considerados de risco baixo (classe 2), enquanto 36,29% foram classificados de risco moderado (classe 3) e 46,72% como risco alto (classe 4). Essas constatações indicam que o índice de risco de incêndio fornece um parâmetro adequado e eficaz para a avaliação espacial da distribuição dos eventos de queimadas ou incêndios florestais no município de Rio Verde.

Palavras-chave: queimadas; modelagem de risco; vegetação; sensoriamento remoto.

¹Instituto Federal de Educação, Ciência e Tecnologia Goiano – Rio Verde (GO), Brazil.

²Universidade de Cuiabá – Cuiabá (MT), Brazil.

Corresponding author: Lucas Soares da Silva Aires – Instituto Federal de Educação, Ciência e Tecnologia Goiano – Rua do Bálsamo, Quadra 55, Lote 1311 – Gameleira I – CEP: 75906-765 – Rio Verde (GO), Brazil. E-mail: lucasaireseng@gmail.com

Conflicts of interest: the authors declare no conflicts of interest.

Funding: none.

Received on: 05/11/2024. Accepted on: 10/26/2024.

<https://doi.org/10.5327/Z2176-94782006>



This is an open access article distributed under the terms of the Creative Commons license.

Introduction

Wildfires result in the uncontrolled burning of biomass, which generates intense heat, and can be extremely harmful to local biodiversity, agricultural operations, and hydrological and carbon cycles (Tomar et al., 2021). These impacts can reduce the capacity of a forest to support life, and the ability of the soil to assimilate new species (Razavi-Termeh et al., 2020). Repeated wildfires over different cycles of drought can induce definitive loss of the genetic heritage of a region, resulting in profound changes in its landscape (Ghorbanzadeh et al., 2019a; Vallejo-Villalta et al., 2019).

Another type of impact caused by wildfires is their capacity to alter the local climate, often negatively, and contribute to regional processes or even global climate change, depending on their magnitude (Singh, 2022). Wildfires play a significant role in global warming, primarily through the release of greenhouse gases into the atmosphere, particularly carbon dioxide (CO₂), methane (CH₄), and nitrous oxide (N₂O) (Pereira et al., 2021). Once liberated from the biomass, these gases contribute to the retention of heat and increase in the temperature of the lower layer of the atmosphere (Mansoor et al., 2022).

A systematic understanding of the consequences of wildfires for the environment and local economies is fundamental to establishing adequate measures of fire prevention, control, and combat (Mohajane et al., 2021). Vettorazzi and Ferraz (1998) developed an approach for mapping fire risk based on a scale of incidence, derived from the factors that determine the occurrence of wildfires. This zoning can be described as the representation of the target region, which is subdivided into specific areas according to the relative importance of the factors and their overall potential for the occurrence and propagation of wildfires (Argañaraz et al., 2018). This mapping permits the visualization of the spatial distribution of fire risk within the target region, which also supports the implementation of adequate measures of control and prevention that are proportional to the risk (Ghorbanzadeh et al., 2019a).

The mapping of fire risk is based on the assumption that several different factors contribute to the probability of ignition of a wildfire and other factors that are related to the propagation of the fire (Vallejo-Villalta et al., 2019; Pourghasemi et al., 2020). These factors are of three types—biological (land cover and use), physical (orientation of the relief and its slope), and socioeconomic, that is, population density and the proximity of homes, and the road network (Juvanhol et al., 2015; Tomar et al., 2021).

The Cerrado savanna of Central Brazil is one of the country's biomes that is most affected by fire, with approximately 63 thousand heat spots detected by remote sensing in 2020 alone (INPE, 2021). The state of Goiás was responsible for 5,730 of these heat spots, that is, 9% of the total, the fourth highest number recorded in the 12 Brazilian states in which the Cerrado is distributed, only behind three states in which the burning of forest for the installation of pasture is particularly intense. In Goiás, the municipality of Rio Verde had the third-highest number of heat spots, with 201 cases recorded in 2020 alone (INPE, 2021).

Rio Verde is known as the capital of Goiás' agribusiness, and is the state's principal producer of grains, with an output of some 3.76 million tons in 2020, representing 14% of the total production of the state (IBGE, 2020). In regions such as Rio Verde, accurate information on fire risk is of paramount importance, given the potential damage that wildfires can cause to the municipality's agribusiness infrastructure (Mohammad et al., 2023).

The mapping of fire risk in the municipality will provide valuable insights for the implementation of adequate decision-making for strategic territorial planning (Novo et al., 2020; Lamat et al., 2021). This information can be used by public organs, such as fire departments, the municipal government, or private entities involved in the management of agribusiness operations, for example (Mohajane et al., 2021). This would allow the authorities to implement the most effective possible management of the resources available to combat wildfires (Pradeep et al., 2022), as well as support the development of strategies for the allocation of teams and resources, continuous monitoring, and campaigns of public awareness that educate local communities on the importance of fire prevention. Together, these measures should guarantee a rapid response, enabling the mitigation of adverse effects on the climate, agribusiness, and biodiversity (Parajuli et al., 2020).

The principal approaches applied to the mapping of fire risk include the analytical hierarchy process (AHP), fuzzy AHP (F-AHP), and logistic regression (Nikhil et al., 2021; Pradeep et al., 2022; Sinha et al., 2023). The AHP consists of a multi-criterion decisionmaking procedure that organizes the risk factors in a hierarchical structure, allowing for systematic comparisons (Lamat et al., 2021). This approach is highly adaptable to different regions and specific contexts and permits the comparison of different scenarios of risk (Nikhil et al., 2021).

The F-AHP, in turn, permits more precise mapping adapted to specific local features and the intrinsic uncertainties of wildfires (Sakellariou et al., 2020). Its purpose is often to mitigate the low flexibility of traditional AHP, especially when there is uncertainty in the weights assigned to different risk criteria (Tabibian, 2022). In particular, the F-AHP is highly sensitive to minor shifts in its assessments, which may lead to unsatisfactory results (Feizizadeh et al., 2023).

The logistic regression approach is also an effective tool for the mapping of fire risk. It permits the prediction of probabilities based on an ample range of variables, with considerable flexibility and easily-interpreted results (Milanović et al., 2020). However, this approach assumes that a linear relationship exists between the variables, which is not often the case when considering the factors that determine the risk of wildfires (Zhang et al., 2022).

In this context, the present study assessed the most relevant factors necessary for the mapping of the fire risk within Rio Verde. An index was developed for the study area based on the AHP approach, given its adaptability, with the distribution of this index being compared with the heat spot data compiled by the Moderate Resolution Imaging Spec-

troradiometer (MODIS) sensor of the AQUA and TERRA satellites between 2005 and 2020.

Methods

Study area

The study area is the municipality of Rio Verde in the Brazilian state of Goiás (Figure 1). This municipality is located in Southwestern Goiás, approximately 231 Southwest of the state capital, Goiânia. The centroid of the urban zone of the municipality is located at 17°43'53" S, 50°35'18" W (IBGE, 2022).

The study area covers 8,379.661 km². The predominant vegetation type in the region is Cerradão woodland, which is a forest formation with sclerophyllous and xeromorphic characteristics, with tree heights of up to 15 m (Santos et al., 2024).

Acquisition of the orbital, spatial, and demographic data

The data on the orientation and slope of the relief were extracted from a digital elevation model (DEM), obtained from the ALOS satellite. These data were acquired from the Alaska Satellite Facility (ASF) platform, which is managed by the National Aeronautics and Space Administration (NASA). This platform generates products corrected geometrically and radiometrically by the synthetic aperture radar

(SAR), with the data being presented in the GeoTIFF format (Polidori, 2024).

Data on population density were obtained based on the census parameters established by the Brazilian Institute of Geography and Statistics (IBGE, 2010), which are available in shapefile format. The number of individuals per private residence or the resident population in private residences used for parameter analysis, was obtained in spreadsheet format (IBGE, 2020).

Factors that influence the risk of wildfires

Three types of factors were selected for the assessment of fire risk within the study area, considering the region's unique features. These were biological (land cover and use), physical (orientation of the relief and slope of the land), and socioeconomic factors (population density and proximity of homes, and the road network).

Biological factors — land use and cover

The condition classification model was carried out using samples of areas that had characteristics within the rules related to specified soil cover. One class is native vegetation (VEG), a category that includes natural arboreal vegetation at different stages of growth, i.e., secondary and climax. The second class is farmland (FAR), which comprises plantations of annual and perennial crops, and cattle pasture.

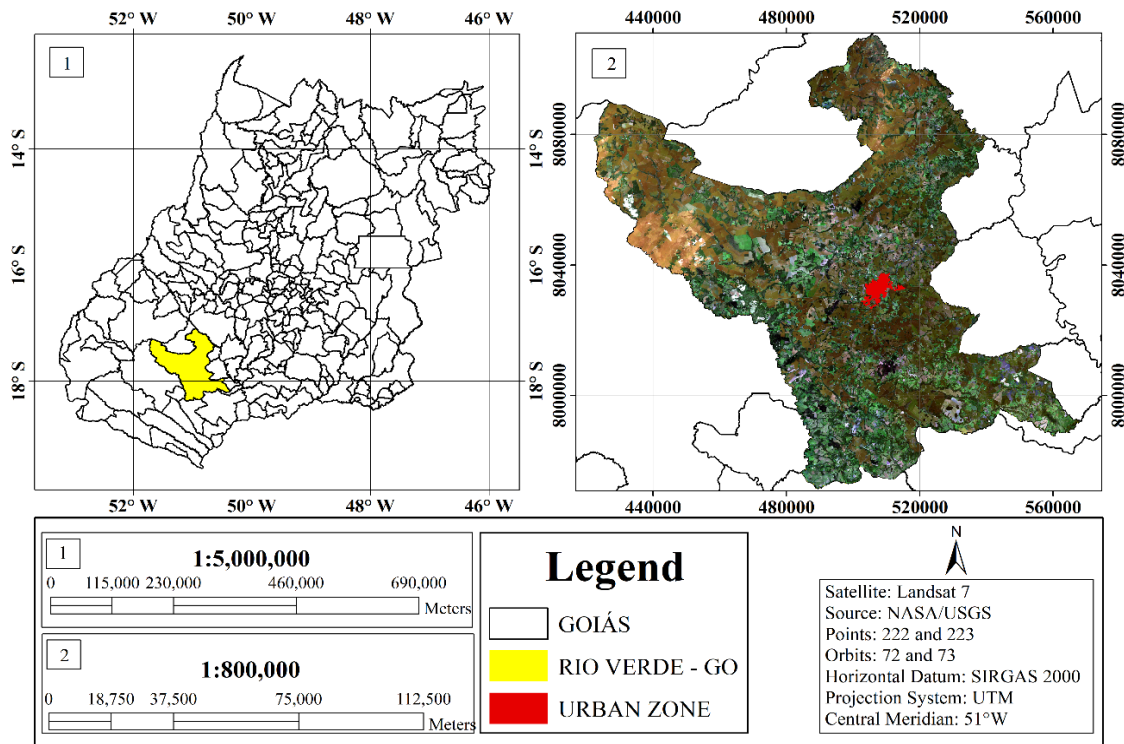


Figure 1 – Location of the study area in the municipality of Rio Verde, in the state of Goiás, in Central Brazil.
Source: Aires and Angelini (2022).

The third, exposed soil (EXS), consists of farmland that has been plowed or otherwise prepared for planting, as well as built infrastructure (houses, buildings), which has a similar profile of surface reflectance. The fourth class is water (WAT), which covers water bodies and associated areas.

The next step was to identify control areas that correspond to these classes. These reference areas were selected based on the visual interpretation of specific areas using the Google Earth tool, for which images obtained between June and September 2020, were adjusted. This procedure was used to determine the limits (maximum and minimum) of the different parameters used to classify the different land use classes (Figure 2). The classes were validated based on a confusion matrix, which assessed the quality of the images' classification based on a comparison with the reference data (Fielding and Bell, 1997; Tremea et al., 2020).

The VEG areas were then reclassified with a coefficient of 1, while FAR was reclassified with a coefficient of 5, and EXS, a coefficient of 6. As they pose no fire risk, WAT areas were reclassified as 0.

Physical factors — slope

Lands that are relatively steeply sloping tend to have a greater potential risk of wildfire than more gently sloping areas (Vallejo-Villalta et al., 2019). The slope of the land was evaluated through DEM images obtained by the ALOS satellite using the PALSAR microwave sensor,

which were analyzed using geoprocessing tools (the slope algorithm) to verify the slope of the land across the different areas of the study municipality (Liao et al., 2020; JAXA, 2022). The slope algorithm can be used to calculate the slope of a terrain based on the adjustment rate of elevation from one DEM cell to the next (Shi et al., 2019).

For the assessment of fire risk, the slope of the different areas was allocated to one of five categories (Figure 3): i. gently sloping (0–5°), with a reclassification coefficient=1; ii. sloping (5–15°), reclassification coefficient=2; iii. substantial sloping (15–25°), reclassification coefficient=3; iv. steep (25–35°), reclassification coefficient=5; and v. very steep (>35°), reclassification coefficient=7 (Santos et al., 2015; Vallejo-Villalta et al., 2019).

Physical factors — orientation of the relief

The orientation of the relief assessment was based on the DEM images obtained by the ALOS satellite using the PALSAR microwave sensor, which were analyzed using remote sensing tools (the hillshade algorithm) to determine the shading conditions of each target area (Liao et al., 2020; JAXA, 2022). The differences in the altitude between triangulable points can be exploited to determine the shading of an area relative to solar radiation, based on the inclination of the terrain (Guth and Kane, 2021).

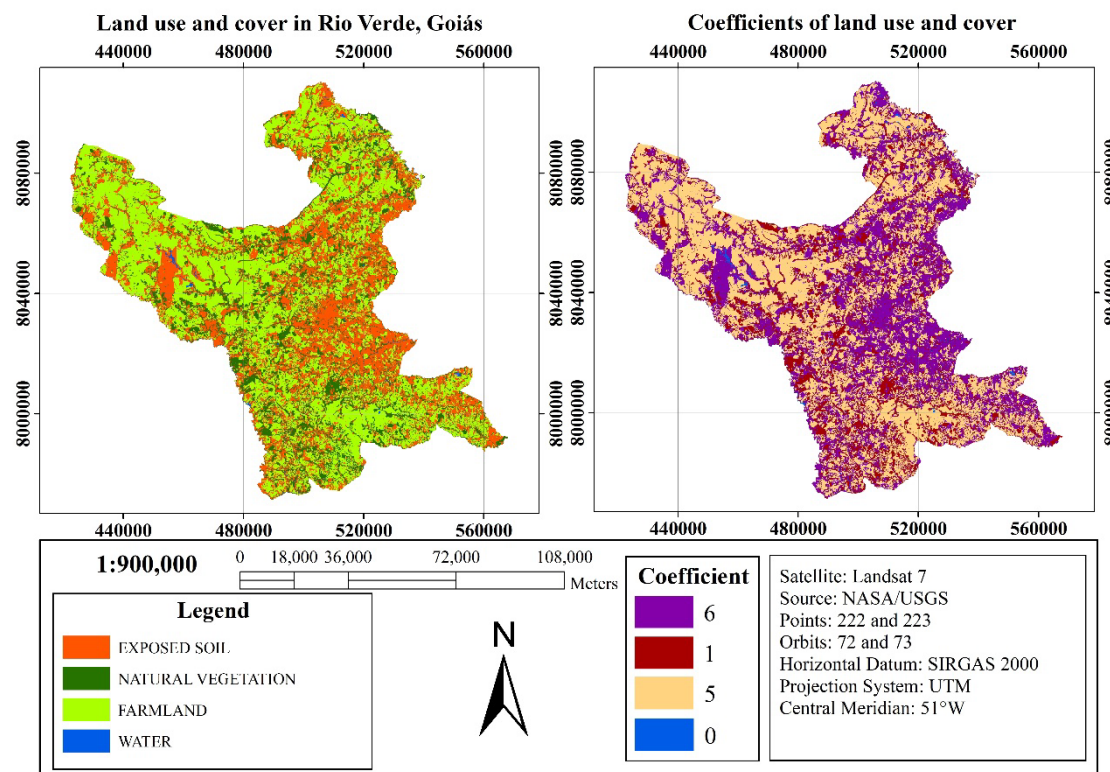


Figure 2 – Classification of land use and cover in the municipality of Rio Verde, in Goiás, Central Brazil, in 2020, and the classification of their areas of influence within the municipality.

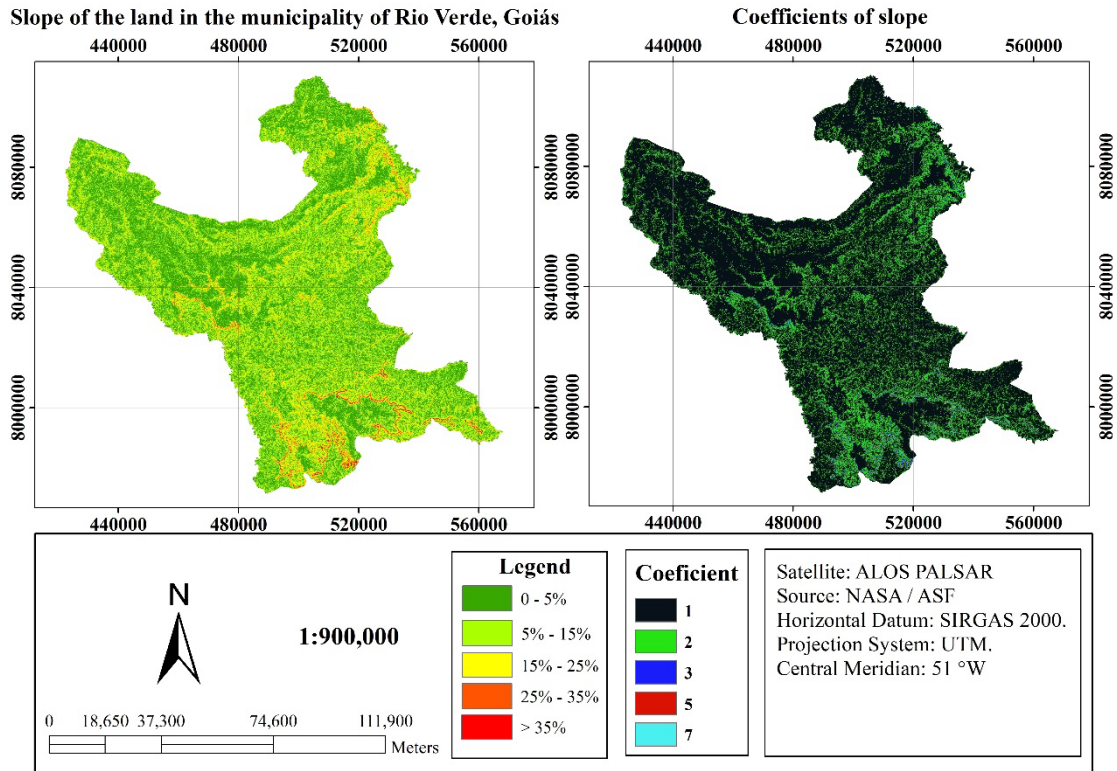


Figure 3 – Slope of the land and classification of its areas of influence within the municipality of Rio Verde, in Goiás, Central Brazil.

The orientation of the relief was assigned to one of six classes of fire risk (Figure 4). These six classes are: i. flat land; ii. fully shaded (112.5–247.5°), with a reclassification coefficient=1; iii. semi-shaded (67.5–112.5°), reclassification coefficient=2; iv. semi-illuminated (22.5–67.5°), reclassification coefficient=3; v. illuminated (247.5–337.5°), reclassification coefficient=5; and vi. fully illuminated (facing North: 337.5–22.5°), reclassification coefficient=7 (Santos, 2015; Ghorbanzadeh et al., 2019a).

Socioeconomic factors — proximity of roads

For the mapping of fire risk, the roads in the study area were divided into two categories: highways and rural roads. The highways are asphalted with at least two lanes and two-way traffic. Four highways were identified in Rio Verde, the BR-60 and BR-452 federal highways, and the GO-333 and GO-174 state highways.

The rural roads, in turn, are all unpaved, subdivided into principal, secondary, and access roads, and internal (farm) tracks. In this classification, the principal roads are wellconstructed thoroughfares with a lane width of at least 5 m. The secondary roads are almost invariably offshoots of the principal roads and responsible for the division of the landscape. The access roads, in turn, are mostly linked to the secondary roads and are responsible for the access to the most internal sections

of the landscape, while the internal tracks link the road system to the infrastructure of the local settlements, farms, and smallholdings.

For the assessment of fire risk, zones of influence of roads were established based on the distance from the target area to the different types of roads. Wherever these zones overlapped, due to the proximity of different road classes, the zone with the highest risk was considered for analysis. This classification (Figure 5) was based on a scale of 500–1500 m, with proximity being defined relative to traffic volume (and the number of persons) expected for each type of thoroughfare. In this case, proximity to a highway was defined as a distance of at least 1500 m, and to a principal road, a distance of at least 1000 m (Chuvieco and Congalton, 1989; Pew and Larsen, 2001; Pourghasemi et al., 2020).

Proximity to a secondary road was defined as a distance of at least 750 m, based on the assumption that these roads tend to have less traffic and fewer people visiting the area, and thus, a lower risk of fire ignition (Juvanhol et al., 2015). Likewise, proximity to an access road was set at 500 m. The Euclidian distance was calculated based on the characteristics of the polyline of the road, delimited by the Pythagoras Theorem, $Hab(Xa, Ya)$ and (Xb, Yb) , for the whole extension of the road (Cavalcante et al., 2019). All areas within a given zone were attributed a reclassification coefficient of 7, while areas not within any of these zones were assigned a coefficient of zero (Table 1).

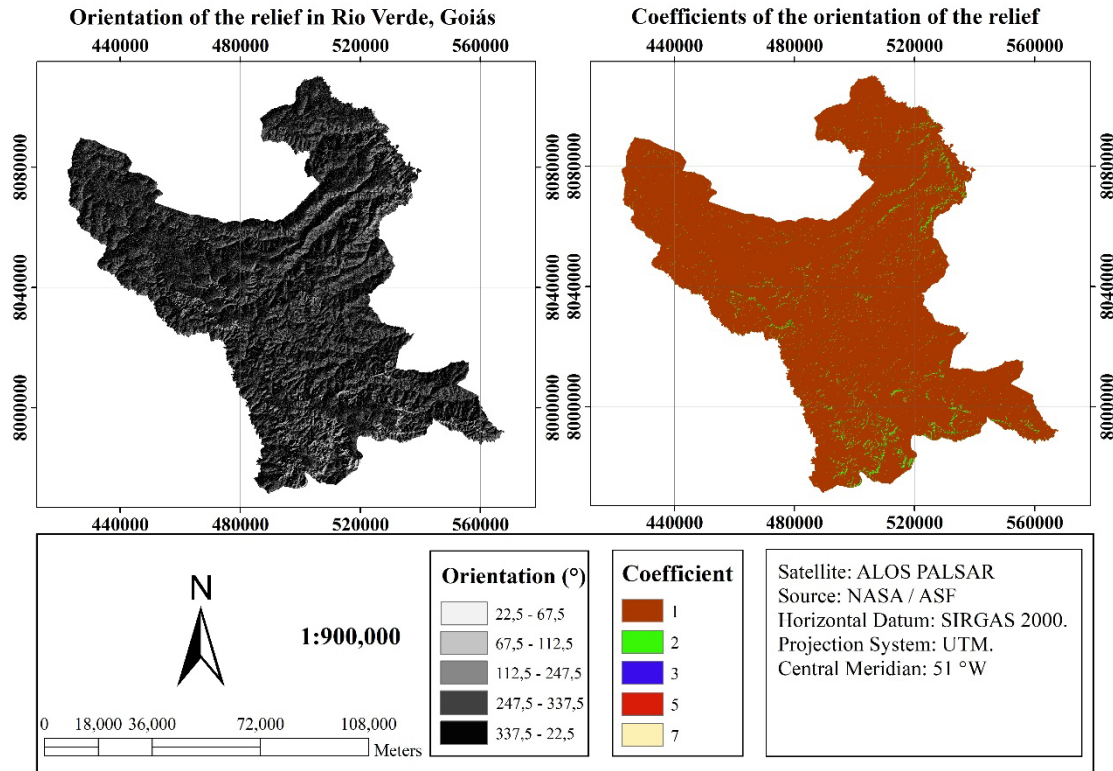


Figure 4 – Orientation of relief and classification of its areas of influence within the municipality of Rio Verde, in Goiás, Central Brazil.

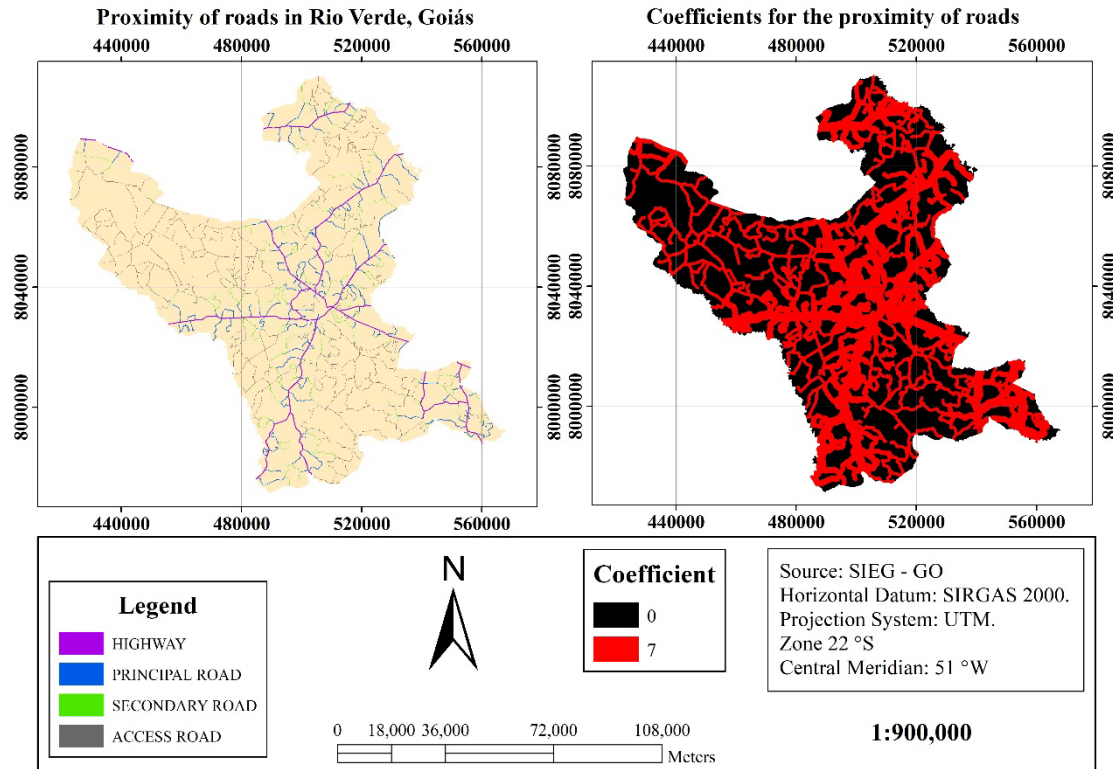


Figure 5 – Distribution of roads and classification of their areas of influence within the municipality of Rio Verde, in Goiás, Central Brazil.

Table 1 – The different classes of each fire risk factor, their respective levels of fire risk, and the coefficients attributed to each category.

Factor/class	Fire risk	Coefficient
Land use and cover		
Plowed farmland	Very high	6
Farmland and pasture	High	5
Natural vegetation	Low	1
Bodies of water	Very Low	0
Population density		
>30 inhabitants per hectare	Very high	7
10–30 inhabitants per hectare	High	5
1–10 inhabitants per hectare	Moderate	3
0–1 inhabitant per hectare	Low	1
Proximity to residences		
<500 m	Very high	7
500–1000 m	High	5
1000–1500 m	Moderate	3
>1500 m	Low	2
Slope		
Very steep (>35°)	Very high	7
Steep (25–35°)	High	5
Substantial sloping (15–25°)	Moderate	3
Sloping (5–15°)	Low	2
Gently sloping (0–5°)	Low	1
Orientation of the relief		
Full sunlight (337.5–22.5°)	Very high	7
Illuminated (247.5–337.5°)	High	5
Semi-illuminated (22.5–67.5°)	Moderate	3
Semi-shaded (67.5–112.5°)	Low	2
Fully shaded (112.5–247.5°)	Low	1
Proximity of roads		
Highways (1500 m)	Very high	7
Principal roads (1000 m)	Very high	7
Secondary roads (750 m)	Very high	7
Access roads (500 m)	Very high	7
No roads	Null	0

Source: adapted from Juvanhol et al. (2015).

Socioeconomic factors – population density

The number of inhabitants of a given locality is a fundamental determinant of the local fire risk, given that population density has a direct effect on the probability of fire ignitions through human activities. Population density (the number of residents per unit area) was calculated using Equation 1 (Deichmann, 1996).

$$Di = \frac{Pi}{Ai} \quad (1)$$

Where:

Di = population density of i per unit area;

Pi = total population of i ; and

Ai = area of i in the same unit of area (as defined by IBGE for the 2010 Census).

The value of Pi corresponds to the number of individuals per private residence or the resident population in private residences, as recorded in the most recent census. To represent the spatial association between the local population density and the fire risk, the population density map was classified into four categories (Figure 6): i. 0–1 inhabitant per hectare (coefficient=1); ii. 1–10 inhabitants per hectare (coefficient=3); iii. 10–30 inhabitants per hectare (coefficient=5); and iv. >30 inhabitants per hectare (coefficient=7).

Socioeconomic factors — proximity of homes

Mapping the distribution of homes within a study area is fundamentally important for classifying fire risk zones (Milanović et al., 2020). Given this, the distribution of homes within Rio Verde was determined using geoprocessing tools, with distances relative to each target area being used to differentiate the risk of each zone. Wherever these zones overlapped, due to the proximity of homes, the zone with the highest risk was considered for analysis. The four classes were created based on the Euclidian distances (Figure 7): i. <500 m (coefficient=7); ii. 500–1000 m (coefficient=5); iii. 1000–1500 m (coefficient=3); and iv. >1500 m (coefficient=2).

The fire risk index model

Once all relevant variables had been determined, it was possible to map the fire risk within the municipality of Rio Verde. To apply the model, thematic maps were labeled according to the characteristics of each variable. The factors with greater potential for the occurrence of wildfires were given a higher weighting in the model. The different classes of each factor were assigned a degree of fire risk, ranging from very low to very high, based on their sensitivity to wildfire events (Table 1). In Table 1, the factors are ranked with the greatest coefficient attributed to the factors that are most important for the fire risk index, with the respective coefficients of the different classes, allocated according to their sensitivity to the occurrence of fires.

Weighting the indices

In the next stage of the analysis, the variables were assigned appropriate weights using the AHP approach. This method was proposed by Saaty (1977) and involves a multi-criterion analysis in which the assessments of the individual criteria are defined through a synthesis of the decision-making agents (Saranya and Saravanan, 2020). Following this concept, a global measure was compiled for each alternative, with its classification being based on its order of importance.

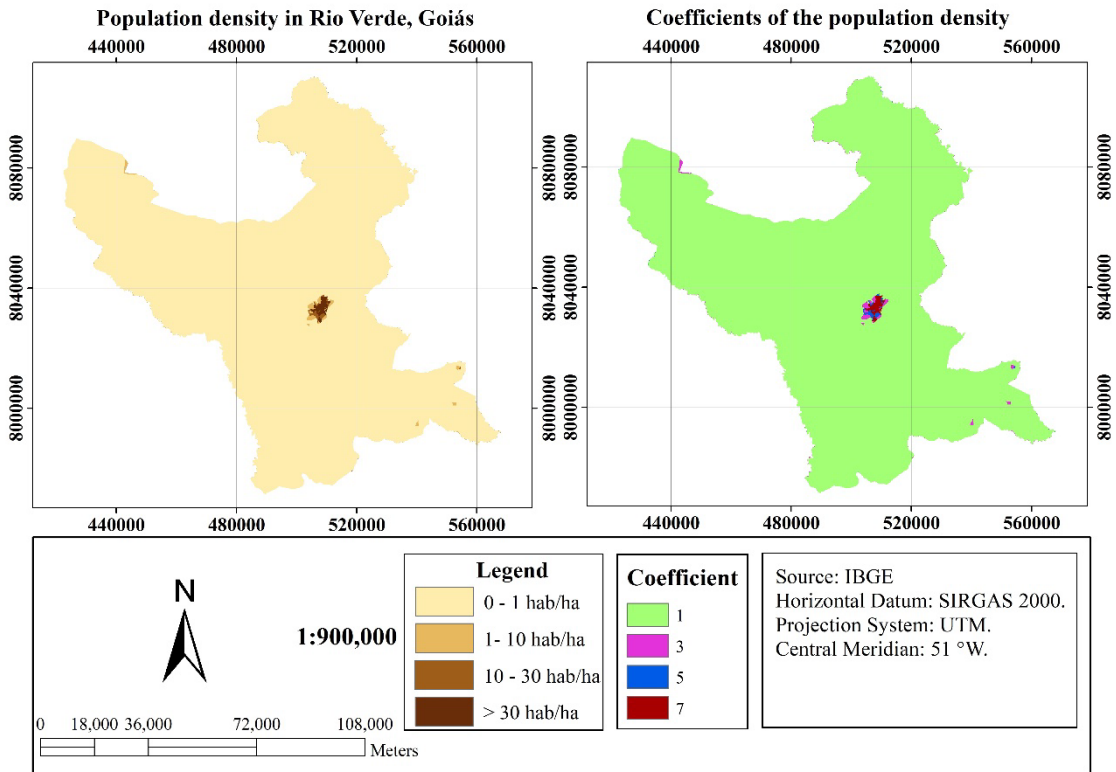


Figure 6 – Distribution of population density and classification of its areas of influence within the municipality of Rio Verde, in Goiás, Central Brazil.

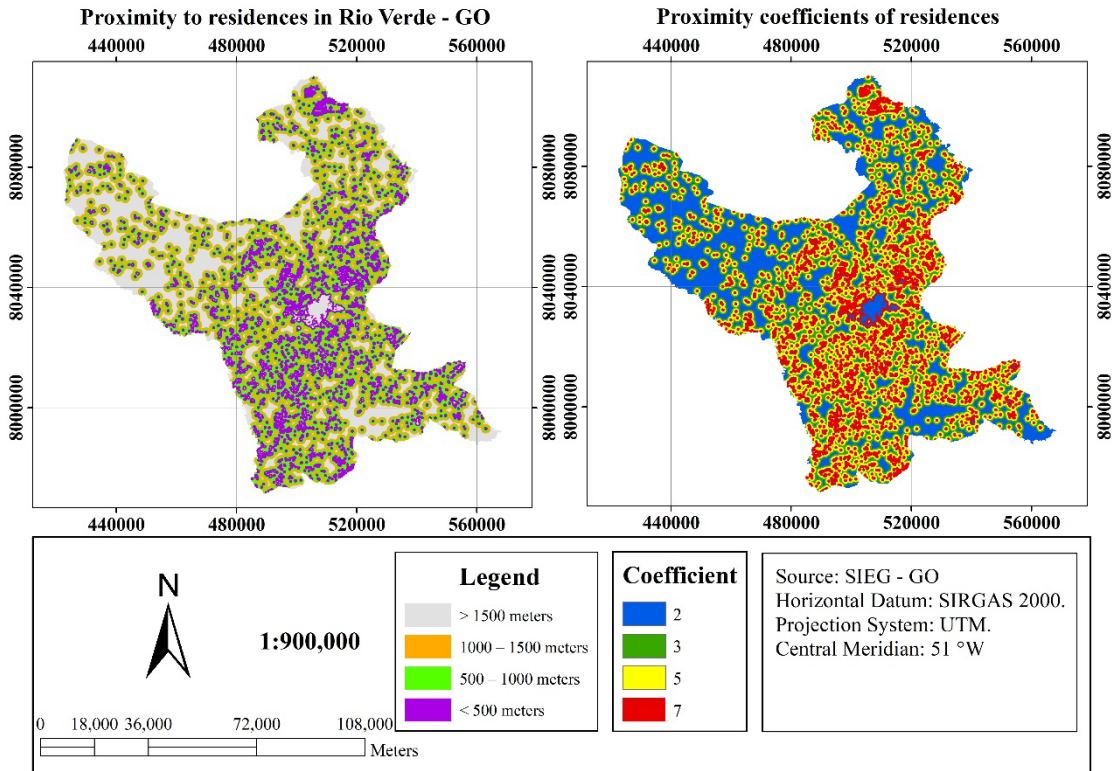


Figure 7 – Distribution of homes and classification of their areas of influence within the municipality of Rio Verde, in Goiás, Central Brazil.

The degree of importance was determined through empirical observation of the intrinsic characteristics of the municipality and the data available in the literature, which were used to compile the decision matrix. The weights were determined on a scale of assessment that varied from 1 to 9; where 1 represents criteria with the same level of importance and 9, an absolute level of importance of one criterion over the other. In general, if the importance of one criterion of X_i in relation to X_j is a_{ij} , that of X_j in relation to X_i will be $1/a_{ij}$.

The relative importance of each factor compared with all the others was estimated based on a comparison matrix, which allowed the decision-making procedure to define a set of relationships among the factors individually. The consistency ratio (CR) was then calculated to evaluate the performance of the weights defined by this procedure. In the assessment scale, values of CR lower than 0.1 indicate a good level of consistency for the weights of each criterion. Whenever this ratio indicated a high level of inconsistency in the comparison of the pair of weights, it was necessary to reevaluate the relationship. The matrix generated here is ordered ($n \times m$) according to the factors analyzed, and is reciprocal and positive, with the principal diagonal equal to 1. The application of the AHP was based on a series of steps, applied to each element of the matrix, for which the following condition must be satisfied (Equation 2):

$$a_{ji} = \frac{1}{a_{ij}} \quad (2)$$

Where:

a = elements of the matrix;

i = line i ; and

j = column j .

The comparisons had the following prerequisite (Equation 3):

$$a_{ij} = \frac{p_i}{p_j} \quad (3)$$

Where:

p_i = degree of importance of the effect of factor of line i on the factor of column j ; and

p_j = degree of importance of the effect of factor of line j on the factor of column i .

After the decision-making process, the comparison matrix A was compiled as follows (Equation 4):

$$A = \begin{pmatrix} \frac{p_1}{p_1} & \dots & \frac{p_1}{p_j} & \dots & \frac{p_1}{p_n} \\ \dots & 1 & \dots & \dots & \dots \\ \frac{p_i}{p_1} & \dots & 1 & \dots & \frac{p_i}{p_n} \\ \dots & \dots & \dots & \dots & \dots \\ \frac{p_n}{p_1} & \dots & \frac{p_n}{p_j} & 1 & \dots \\ \dots & \dots & \frac{p_n}{p_j} & \dots & 1 \end{pmatrix} \quad (4)$$

The weight of each factor can be determined based on matrix A (Equation 4). For this, the elements of column j are added together, as follows (Equation 5):

$$\frac{p_i}{p_j} + \dots + \frac{p_i}{p_j} + \dots + \frac{p_n}{p_n} = \sum_{i=1}^n p_i \quad (5)$$

Column j was then normalized (Equation 6), based on the ratio between Equations 3 and 5:

$$\frac{\frac{p_i}{p_j}}{\sum_{i=1}^n \frac{p_i}{p_j}} = \frac{p_i}{p_j} \cdot \frac{p_j}{\sum_{i=1}^n p_i} = \frac{p_i}{\sum_{i=1}^n p_i} \quad (6)$$

...with the weight of line i (W_i) being calculated by the arithmetic mean of its terms (Equation 7):

$$W_i = \left(\frac{p_i}{\sum_{i=1}^n p_i} + \dots + \frac{p_i}{\sum_{i=1}^n p_i} \right) \cdot \frac{1}{n} \quad (7)$$

The weights were then obtained, beginning with the verification of the consistency of the assessments based on the highest eigenvalue of the comparison matrix. The eigenvalue is calculated by the product of the normalized values (Equation 6) with their respective weights (Equation 7), with the values being summed (Equation 8):

$$\lambda_{max} = \sum_{i=1}^n \left(W_i \cdot \frac{p_i}{\sum_{i=1}^n p_i} \right) \quad (8)$$

Where:

λ_{max} = maximum eigenvalue.

The consistency index (CI) was calculated using Equation 9, following Saaty (1980):

$$CI = \frac{\lambda_{max} - n}{n - 1} \quad (9)$$

Where:

CI = consistency index.

The final step was the calculation of the CR (Equation 10), which is the pairwise CI of the comparison matrix (Saaty, 1980). CR values below 0.1 indicate a lack of inconsistency in the values attributed by the assessment, whereas, once again, values of over 0.1 require a new evaluation.

$$CR = \frac{CI}{RI} \quad (10)$$

Where:

RI = random index.

The RI is a value proposed by Saaty (2005), which varies according to the number of factors evaluated in the construction of the matrix (Table 2).

The multi-criterion AHP was based on the weighted linear combination model. The values obtained by this approach are derived from the standardization of the factors on a common scale, with their respective weights, which are combined in sequence through a weighted mean (Pimenta et al., 2019). The weights obtained by the AHP method permit new values to be attributed to their respective classes (Table 3), and whenever necessary, the weights are modified, before the values are exported to thematic maps (Lamat et al., 2021). In the final step, Equation 11, which was proposed by Santos (2015), was inserted using geographic information system (GIS) data processing tools to extract the fire risk indices for the municipality of Rio Verde.

$$FRI = PXR.PXR_{pi} + PXH.PXH_{pi} + LUC.LUC_{pi} + POD.POD_{pi} + ORI.ORI_{pi} + SLO.SLO_{pi} \quad (11)$$

Where:

FRI = fire risk indices; and

pi = the statistical weight calculated for each factor.

Results and Discussion

Mapping of the factors

The mapping of land use in the study area in 2020 (Figure 2) revealed a predominance of active farmland (coefficient 5) and exposed soil (coefficient 6). The slope of the land was predominantly discreet, mostly below 15%, being represented by coefficients 1 and 2 (Figure 3). Similarly, the orientation of the relief was predominantly assigned to the semi-shaded and fully shaded classes, with coefficients of 1 and 2 (Figure 4).

Table 2 – Values of the random index proposed by Saaty (2005) for matrices of different sizes.

Number of factors	1	2	3	4	5	6	7	8
Random index	0.00	0.00	0.58	0.89	1.12	1.32	1.41	1.41

Table 3 – Number of classes considered for each factor analyzed in this stud, used to determine the fire risk index.

Factor	Code	Number of classes
Land use and cover	LUC	k=4
Population density	POD	l=4
Proximity of homes	PXH	j=2
Slope	SLO	n=5
Orientation of the relief	ORI	m=6
Proximity of roads	PXR	i=4

Source: the authors (2022).

In terms of proximity of roads, highways clearly have a major influence, given that they affect areas within a radius of 1500 m (Figure 5). The population density was concentrated within the urban zone of the municipality, as well as a few other isolated points, primarily in the Southwest of the municipality, where coefficients 5 and 7 predominated (Figure 6).

Determination of the weights of the study factors

It was possible to determine the weight of each factor included in the comparison matrix (Table 4). The CR value recorded herein was 0.0190, which is well below the threshold of 0.100 established by Saaty (1980). Following the substitution of the weights, it was possible to define Equation 12, which was used to calculate the fire risk index.

$$FRI = 0.3035.PXR + 0.3035.PXH + 0.1903.LUC + 0.1087.POD + 0.0519.ORI + 0.0421.SLO \quad (12)$$

Mapping the fire risk of the study area

Based on the integrated analysis of all the different factors that make up the spatial variables considered in this study in terms of the probability of the ignition and perpetuation of a wildfire, it was possible to map the fire risk index for the municipality of Rio Verde in the Brazilian state of Goiás (Figure 8). The fire risk index was determined through Equation 12 in the GIS environment. For mapping, the index was divided into five classes: i. water; ii. low risk; iii. moderate risk; iv. high risk; and v. very high risk.

The areas associated with bodies of water in Rio Verde covered 3,489.57 hectares, which is equivalent to 0.410% of the total area of the state. This type of land cover has a negligible risk of ignition, given the minimal capacity of this environment for combustion (Pourghasemi et al., 2020). The low-risk areas (class 2) covered 173,428.62 hectares, which is equivalent to 20.697% of the total area of the municipality. These low-risk areas tend not to be located within the zone of influence of any of the factors with relatively high weights for the occurrence of fires, such as PXH and PXR.

Table 4 – Pairwise comparison matrix and the respective weights of the factors that influence the fire risk of the study area.

Factor	SLO	ORI	POD	LUC	PXH	PXR	Weight
SLO	1	1	1/3	1/5	1/7	1/7	0.0421
ORI	1	1	1/3	1/3	1/5	1/5	0.0519
POD	3	3	1	1/3	1/3	1/3	0.1087
LUC	5	3	3	1	1/2	1/2	0.1903
PXH	7	5	3	2	1	1	0.3035
PXR	7	5	3	2	1	1	0.3035
CR	0.0190						

LUC: land use and cover; POD: population density; PXH: proximity to homes; SLO: slope; ORI: orientation of the relief; PXR: proximity of roads; CR: consistency ratio.

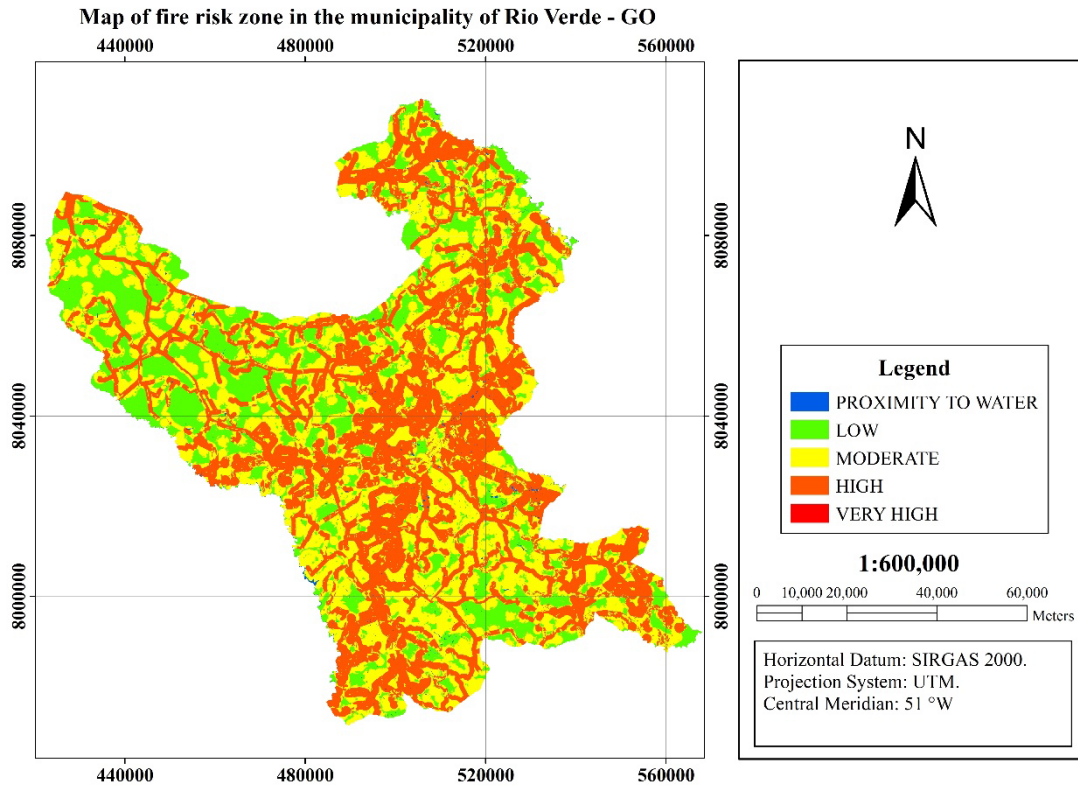


Figure 8 – Distribution of fire risk zones within the municipality of Rio Verde, Goiás, Central Brazil.

One other factor that had a major influence here was LUC, which were primarily VEG and, principally, FAR—categories that have a lower fire risk.

Areas of moderate risk (class 3) occupied 313,502.09 hectares, the equivalent to 41.332% of the municipality area. These areas were influenced primarily by the distribution of homes within the municipality. Given the increased human presence in these areas, there is a greater probability of a wildfire ignition (Buschinelli and Costa, 2020; Oliveira et al., 2020). Another factor that had a strong influence on this configuration was the LUC in the areas surrounding these homes, which were typically occupied by agribusiness, in particular, EXS. The biomass of many cash crops has a high risk of combustion, with a marked potential for the generation of extensive wildfires (Razavi-Termeh et al., 2020). Moro and Oliveira (2023) georeferenced the data on wildfires from case reports registered in the South of the Brazilian state of Espírito Santo, and estimated that more than 48% of the events were recorded in urban areas, which further reinforces the apparent human influence on the occurrence of controlled burns.

Physical factors, that is, SLO and ORI of the terrain, and their distribution within the municipality, are also important here, being the classes that most influence the potential for wildfires, distributed primarily in the Central-Southern portion of the municipality (Vallejo-Villalta et al., 2019; Novo et al., 2020). This is where the largest

proportion of the areas classified as moderate and high (class 4) risk for the occurrence and propagation of wildfires were located.

The high-risk areas (class 4) covered a total of 346,339.59 hectares, which is 41.332% of the total area of the municipality. These areas are influenced primarily by the distribution of roads within the municipality, which generate zones of constant transit, with the flux of persons in the area increasing the probability of the ignition of a fire (Ghorbanzadeh et al., 2019a; Mohajane et al., 2021). Once again, the LUC has a major influence on this configuration, given that the areas neighboring roads tend to be occupied by agribusiness, in particular by EXS. Areas of very high risk (class 5) were negligible; however, accounting for only 0.001% of the total area of the municipality (Table 5).

Comparative analysis of the heat spots detected in the municipality of Rio Verde over sixteen years between 2005 and 2020

The fire risk map (Figure 8) was systematically compared with the distribution of heat sources detected in Rio Verde, to determine the overlap between the distribution of the different fire risk zones and the heat sources detected by the MODIS satellite sensor AQUA and TERRA from 2005 to 2020. In broad terms, there was a progressive increase in the proportion of heat spots with increasing fire risk (Table 6).

Table 5 – Distribution of the different classes of the fire risk index in the municipality of Rio Verde, Goiás, Brazil, based on the analysis conducted in the present study.

Risk class	Fire risk index	Degree of risk	Area in hectares (% of the study area)
1	– (water)	Very low	3489.57 (0.410)
2	0–2	Low	173,428.62 (20.697)
3	2–4	Moderate	313,502.09 (37.413)
4	4–6	High	346,339.59 (41.332)
5	>6	Very high	11.85 (0.001)

Table 6 – Distribution of the heat spots in Rio Verde recorded by the MODIS satellite sensor AQUA and TERRA, from 2005 to 2020, among the different zones of fire risk established by the analysis of different risk factors identified in the present study.

Risk class	Fire Risk Index	Degree of risk	Number (%) of heat spots
1	–	Very low	27 (0.645)
2	0–2	Low	684 (16.363)
3	2–4	Moderate	1517 (36.291)
4	4–6	High	1953 (46.722)
5	>6	Very high	0 (0.000)
Total			4180 (100.000)

This comparative analysis showed that only ten heat spots (0.645% of the total) were detected in the lowest risk areas, i.e., bodies of water (class 1). These areas have a negligible risk of ignition, given their extremely low capacity for combustion, as reflected in the small number of heat spots detected (Pourghasemi et al., 2020).

A total of 684 heat spots were detected within the low-risk areas (class 2), which is equivalent to 16.363% of the municipality. These areas have low population density, relatively few roads, more level relief, and land use and cover with reduced capacity for the production of biomass as fuel, all of which reduce the chances of combustion (Ghorbanzadeh et al., 2019b; Vallejo-Villalta et al., 2019; Novo et al., 2020; Scholtz et al., 2020).

The areas of moderate risk (class 3) had 1,517 heat spots, just over a third (36.291%) of the total. In this case, the proximity of homes was an important factor, given that the local concentration of residences maximizes the chances of human contact in the area (Oliveira et al., 2020). The largest number of heat spots, that was 1,953 (46.722% of the total), was detected within the high-risk (class 4) areas that are influenced primarily by factors of higher weights, such as PXH and PXR, which are related directly to human contact, amplifying the number of wildfires or controlled burns (Ghorbanzadeh et al., 2019b; Vallejo-Villalta et al., 2019). No heat spots were detected in any of the very high-risk (class 5) areas, probably because of their greatly reduced extent (Table 5).

Conclusions

The results of the present study demonstrated clearly that the compilation of the fire risk index was an adequate and effective approach for the assessment of wildfire distribution in Rio Verde. Overall, the areas of high risk covered the largest part of the municipality.

The moderate risk zones covered the second largest area in the municipality, and were influenced primarily by the presence of homes, which tends to maximize the chances of human contact. The low-risk zones made up only the third largest area of the municipality.

Authors' contributions

Aires, L.S.S.: conceptualization, data curation, formal analysis, investigation, methods, project administration, resources, software, validation, visualization, writing – original draft, writing – review & editing. **Angelini, A.P.:** conceptualization, formal analysis, investigation, methods, project administration, resources, supervision, validation, visualization, writing – original draft, writing – review & editing. **Danelichen, V.H.M.:** supervision, validation, visualization, writing – review & editing.

References

- Aires, L.S.; Angelini, L.P. Avaliação espaço-temporal de focos de calor no sudoeste do estado de Goiás, Brasil. *Revista Brasileira de Geografia Física*, v. 15 (06), 3136-3155, 2022.
- Argañaraz, J.P.; Landi, M.A.; Scavuzzo, C.M.; Bellis, L.M., 2018. Determining fuel moisture thresholds to assess wildfire hazard: A contribution to an operational early warning system. *PLOS One*, v. 13 (10), e0204889. <https://doi.org/10.1371/journal.pone.0204889>.
- Buschinelli, C.C.A.; Costa, B.M.R., 2020. Expansão da silvicultura no Brasil Central: estudo de caso em Rio Verde (GO). *Embrapa Meio Ambiente-Boletim de Pesquisa e Desenvolvimento (INFOTECA-E)*, [S.l.] (Accessed February 13, 2023) at: <https://www.infoteca.cnptia.embrapa.br/infoteca/handle/doc/1126480>.
- Cavalcante, R.N.B.; Sousa, M.H.R.; Sousa, J.P.R., 2019. A interdisciplinaridade entre matemática e geografia: inferindo conceitos de localização e distâncias na cidade. *Revista Encantar-Educação, Cultura e Sociedade*, v. 1 (3), 07-20. (Accessed April 25, 2023) at: <https://www.homologacao.revistas.uneb.br/index.php/encantar/article/view/8150>.
- Chuvieco, E.; Congalton, R.G., 1989. Application of remote sensing and geographic information systems to forest fire hazard mapping. *Remote sensing of Environment*, v. 29 (2), 147-159. [https://doi.org/10.1016/0034-4257\(89\)90023-0](https://doi.org/10.1016/0034-4257(89)90023-0).
- Deichmann, U., 1996. A review of spatial population database design and modeling. National Center for Geographic Information and Analysis, Santa Barbara, 58 p (Accessed October 16, 2023) at: <https://escholarship.org/uc/item/6g190671>.

- Feizizadeh, B.; Omarzadeh, D.; Mohammadnejad, V.; Khallaghdi, H.; Sharifi, A.; Golmohamadzadeh Karkarg, B., 2023. An integrated approach of artificial intelligence and geoinformation techniques applied to forest fire risk modeling in Gachsaran, Iran. *Journal of Environmental Planning and Management*, v. 66 (6), 1369-1391. <https://doi.org/10.1080/09640568.2022.2027747>.
- Fielding, A.H.; Bell, J.F., 1997. A review of methods for the assessment of prediction errors in conservation presence/absence models. *Environmental Conservation*, v. 24, 38-49. <https://doi.org/10.1017/S0376892997000088>.
- Ghorbanzadeh, O.; Blaschke, T.; Gholamnia, K.; Aryal, J., 2019a. Forest fire susceptibility and risk mapping using social/infrastructural vulnerability and environmental variables. *Fire*, v. 2 (3), 50. <https://doi.org/10.3390/fire2030050>.
- Ghorbanzadeh, O.; Valizadeh Kamran, K.; Blaschke, T.; Aryal, J.; Naboureh, A.; Einali, J.; Bian, J., 2019b. Spatial prediction of wildfire susceptibility using field survey gps data and machine learning approaches. *Fire*, v. 2 (3), 43. <https://doi.org/10.3390/fire2030043>.
- Guth, P.; Kane, M., 2021. Slope, aspect, and hillshade algorithms for non-square digital elevation models. *Transactions in GIS*, v. 25 (5), 2309-2332. <https://doi.org/10.1111/tgis.12852>.
- Instituto Brasileiro de Geografia e Estatística (IBGE), 2010. Downloads. *Censo_Demográfico_2010* (Accessed January 16, 2021) at: <https://www.ibge.gov.br/estatisticas/downloads-estatisticas.html>.
- Instituto Brasileiro de Geografia e Estatística (IBGE), 2020. Rio Verde (Accessed January 9, 2022) at: <https://cidades.ibge.gov.br/brasil/go/rio-verde/pesquisa>.
- Instituto Brasileiro de Geografia e Estatística (IBGE), 2022. Organização do território. *Malhas territoriais* (Accessed August 30, 2021) at: <https://www.ibge.gov.br/geociencias/organizacao-do-territorio/malhas-territoriais>.
- Instituto Nacional de Meteorologia (INMET), 2021. Banco de Dados Meteorológico para Ensino e Pesquisa - BDMEP. INMET, Brasília (Accessed January 14, 2020) at: .
- Instituto Nacional de Pesquisas Espaciais (INPE), 2021. INPE Programa Queimadas - BD Queimadas. Rio Verde – GO (Accessed January 14, 2021) at: .
- Japan Aerospace Exploration Agency (JAXA), ano. ALOS Data Users Handbook (Accessed May 16, 2022) at: https://www.eorc.jaxa.jp/ALOS/en/doc/fdata/ALOSHB_RevC_EN.pdf.
- Juvanhol, R.S.; Fiedler, N.C.; Santos, A.R., 2015. Modelagem de risco de incêndios em florestas naturais com o uso de geotecnologias. Santos, A.R.; Ribeiro, C.A.A.S.; Peluzio, J.B.E., *Geotecnologias & Análise Ambiental*. Alegre: Centro de Ciências Agrárias, Universidade Federal do Espírito Santo, pp. 160-172. Available at: <https://www.mundogeomatica.com/Publicacoes/Capitulo23.pdf>
- Lamat, R.; Kumar, M.; Kundu, A.; Lal, D., 2021. Forest fire risk mapping using analytical hierarchy process (AHP) and earth observation datasets: A case study in the mountainous terrain of Northeast India. *SN Applied Sciences*, v. 3 (4), 425. <https://doi.org/10.1007/s42452-021-04391-0>.
- Liao, Z.; Van Dijk, A.I.J.M.; He, B.; Rozas Larraondo, P.; Scarth, P.F., 2020. Woody vegetation cover, height and biomass at 25-m resolution across Australia derived from multiple site, airborne and satellite observations. *International Journal of Applied Earth Observation and Geoinformation*, v. 93, 102209. <https://doi.org/10.1016/j.jag.2020.102209>.
- Mansoor, S.; Farooq, I.; Kachroo, M.M.; Mahmoud, A.E.D.; Fawzy, M.; Popescu, S.M.; Alyemeni, M.N.; Sonne, C.; Rinklebe, J.; Ahmad, P., 2022. Elevation in wildfire frequencies with respect to the climate change. *Journal of Environmental Management*, v. 301, 113769. <https://doi.org/10.1016/j.jenvman.2021.113769>.
- Milanović, S.; Marković, N.; Pamučar, D.; Gigović, L.; Kostić, P.; Milanović, S.D., 2020. Forest fire probability mapping in eastern Serbia: Logistic regression versus random forest method. *Forests*, v. 12 (1), 5. <https://doi.org/10.3390/f12010005>.
- Mohajane, M.; Costache, R.; Karimi, F.; Pham, Q.B.; Essahlaoui, A.; Nguyen, H.; Laneve, G.; Oudija, F., 2021. Application of remote sensing and machine learning algorithms for forest fire mapping in a Mediterranean area. *Ecological Indicators*, v. 129, 107869. <https://doi.org/10.1016/j.ecolind.2021.107869>.
- Mohammad, L.; Bandyopadhyay, J.; Sk, R.; Mondal, I.; Nguyen, T.T.; Lama, G.F.C.; Tran Anh, D., 2023. Estimation of agricultural burned affected area using NDVI and dNBR satellite-based empirical models. *Journal of Environmental Management*, v. 343, 118226. <https://doi.org/10.1016/j.jenvman.2023.118226>.
- Moro, I.P.; Oliveira, F., 2023. Gestão de combate a incêndios: distribuição espacial e temporal no sul do estado do Espírito Santo. *Revista do Serviço Público*, v. 74 (4), 846-868. <https://doi.org/10.21874/rsp.v74i4.9887>
- Nikhil, S.; Homian Danumah, J.; Saha, S.; Prasad, M.K.; Ambujendran, R.; Mammen, P.C.; Ajin, R.S.; Kuriakose, S.L., 2021. Application of GIS and AHP method in forest fire risk zone mapping: a study of the Parambikulam tiger reserve, Kerala, India. *Journal of Geovisualization and Spatial Analysis*, v. 5 (1), 14. <https://doi.org/10.1007/s41651-021-00082-x>.
- Novo, A.; Fariñas-Álvarez, N.; Martínez-Sánchez, J.; González-Jorge, H.; Fernández-Alonso, J.M.; Lorenzo, H., 2020. Mapping forest fire risk—a case study in Galicia (Spain). *Remote Sensing*, v. 12 (22), 3705. <https://doi.org/10.3390/rs12223705>.
- Oliveira, V.F.R.; Silva, E.R.S.; Vick, E.P.; Silva, B.H.M. da; Lima, C.G.R.; Bacani, V.M., 2020. Geoprocessamento aplicado ao mapeamento de risco a incêndios. *Revista Brasileira de Geografia Física*, v. 13 (03), 1194-1212. <https://doi.org/10.26848/rbgf.v13.3.p1194-1212>.
- Parajuli, A.; Gautam, A.P.; Sharma, S.P.; Bhujel, K.B.; Sharma, G.; Thapa, P.B.; Bist, B.S.; Poudel, S., 2020. Forest fire risk mapping using GIS and remote sensing in two major landscapes of Nepal. *Geomatics, Natural Hazards and Risk*, v. 11 (1), 2569-2586. <https://doi.org/10.1080/19475705.2020.1853251>.
- Pereira, P.; Bogunovic, I.; Zhao, W.; Barcelo, D., 2021. Short-term effect of wildfires and prescribed fires on ecosystem services. *Current Opinion in Environmental Science & Health*, v. 22, 100266. <https://doi.org/10.1016/j.coesh.2021.100266>
- Pew, K.L.; Larsen, C.P.S., 2001. GIS analysis of spatial and temporal patterns of human-caused wildfires in the temperate rain forest of Vancouver Island, Canada. *Forest ecology and management*, v. 140 (1), 1-18. [https://doi.org/10.1016/S0378-1127\(00\)00271-1](https://doi.org/10.1016/S0378-1127(00)00271-1).
- Pimenta, L.B.; Beltrão, N.E.S.; Gemaque, A.M.S.; Tavares, P.A., 2019. Processo Analítico Hierárquico (AHP) em ambiente SIG: temáticas e aplicações voltadas à tomada de decisão utilizando critérios espaciais. *Interações (Campo Grande)*, v. 20, 407-420. <https://doi.org/10.20435/inter.v20i2.1856>.
- Polidori, L., 2024. Sensoriamento remoto por radar a nível de pós-graduação no Brasil: desafios e soluções. *Revista Presença Geográfica*, v. 11 (1), 14-20. <https://doi.org/10.36026/rpgeo.v11i1.7768>.
- Pourghasemi, H.R.; Gayen, A.; Edalat, M.; Zarafshar, M.; Tiefenbacher, J.P., 2020. Is multi-hazard mapping effective in assessing natural hazards and integrated watershed management. *Geoscience Frontiers*, v. 11 (4), 1203-1217. <https://doi.org/10.1016/j.gsf.2019.10.008>.
- Pradeep, G.S.; Homian Danumah, J.; Nikhil, S.; Prasad, M.K.; Patel, N.; Mammen, P.C.; Rajaneesh, A.; Oniga, V.-E.; Ajin, R.S.; Kuriakose, S.L., 2022. Forest fire risk zone mapping of Eravikulam National Park in India: a comparison between frequency ratio and analytic hierarchy process methods. *Croatian Journal of Forest Engineering: Journal for Theory and Application of Forestry Engineering*, v. 43 (1), 199-217. <https://doi.org/10.5552/crojfe.2022.1137>.

- Razavi-Termeh, S.V.; Sadeghi-Niaraki, A.; Choi, S.-M., 2020. Ubiquitous GIS-based forest fire susceptibility mapping using artificial intelligence methods. *Remote Sensing*, v. 12 (10), 1689. <https://doi.org/10.3390/rs12101689>.
- Saaty, T.L., 1977. A scaling method for priorities in hierarchical structures, *Journal of Mathematical Psychology*, v. 15 (3), 234-281. [https://doi.org/10.1016/0022-2496\(77\)90033-5](https://doi.org/10.1016/0022-2496(77)90033-5).
- Saaty, T.L., 1980. *The analytic hierarchy process*. McGraw-Hill, New York, 278 p. [https://doi.org/10.1016/0270-0255\(87\)90473-8](https://doi.org/10.1016/0270-0255(87)90473-8).
- Saaty, T.L., 2005. *Theory and applications of the analytic network process: decision making with benefits, opportunities, costs, and risks*. RWS Publications, Pittsburgh.
- Sakellariou, S.; Cabral, P.; Caetano, M.; Pla, F.; Painho, M.; Christopoulou, O.; Sfougaris, A.; Dalezios, N.; Vasilakos, C., 2020. Remotely sensed data fusion for spatiotemporal geostatistical analysis of forest fire hazard. *Sensors*, v. 20 (17), 5014. <https://doi.org/10.3390/s20175014>
- Santos, A.R.; Ribeiro, C.A.A.S.; Peluzio, J.B.E.; de Oliveira Peluzio, T.M.; Moreira, G.L.; Magalhães, I.A.L., 2015. *Geotecnologias & Análise Ambiental*. Alegre: Centro de Ciências Agrárias, Universidade Federal do Espírito Santo, Instituto Federal de Educação, Ciência e Tecnologia do Estado do Espírito Santo e Universidade Federal de Viçosa
- Santos, F.F.M.; Durigan, G.; Boschi, R.S.; Ivanauskas, N.; Rodrigues, R.R., 2024. Tree community dynamics in the cerradão (2002-2016): A case of biome shift. *Forest Ecology and Management*, v. 555, 121698. <https://doi.org/10.1016/j.foreco.2024.121698>.
- Saranya, T.; Saravanan, S., 2020. Groundwater potential zone mapping using analytical hierarchy process (AHP) and GIS for Kancheepuram District, Tamilnadu, India. *Modeling Earth Systems and Environment*, v. 6 (2), 1105-1122. <https://doi.org/10.1007/s40808-020-00744-7>.
- Scholtz, R.; Prentice, J.; Tang, Y.; Twidwell, D., 2020. Improving on MODIS MCD64A1 burned area estimates in grassland systems: A case study in Kansas flint hills tall grass prairie. *Remote Sensing*, v. 12 (13), 2168. <https://doi.org/10.3390/rs12132168>.
- Shi, X.; Yang, C.; Zhang, L.; Jiang, H.; Liao, M.; Zhang, L.; Liu, X., 2019. Mapping and characterizing displacements of active loess slopes along the upstream Yellow River with multi-temporal InSAR datasets. *Science of The Total Environment*, v. 674, 200-210. <https://doi.org/10.1016/j.scitotenv.2019.04.140>.
- Singh, S., 2022. Forest fire emissions: a contribution to global climate change. *Frontiers in Forests and Global Change*, v. 5, 925480. <https://doi.org/10.3389/ffgc.2022.925480>.
- Sinha, A.; Nikhil, S.; Ajin, R.S.; Homian Danumah, J.; Saha, S.; Costache, R.; Rajaneesh, A.; Sajinkumar, K.S.; Amrutha, K.; Johny, A.; Marzook, F.; Mammen, P.C.; Abdelrahman, K.; Fnais, M.S.; Abioui, M., 2023. Wildfire risk zone mapping in contrasting climatic conditions: An approach employing AHP and F-AHP models. *Fire*, v. 6 (2), 44. <https://doi.org/10.3390/fire6020044>.
- Tabibian, S., 2022. Physical zoning of forest fire risk using fuzzy AHP and GIS methods (case study: Asalem). *Physical Social Planning*, v. 9 (2), 61-72. <https://doi.org/10.30473/psp.2022.62345.2561>.
- Tomar, J.S.; Kranjčić, N.; Đurin, B.; Kanga, S.; Singh, S.K., 2021. Forest fire hazards vulnerability and risk assessment in Sirmaur district forest of Himachal Pradesh (India): A geospatial approach. *ISPRS International Journal of Geo-Information*, v. 10 (7), 447. <https://doi.org/10.3390/ijgi10070447>.
- Tremea, A.; Gallo, J.; Silva, A.J.F., 2020. Análise espaço-temporal do desmatamento via sensoriamento remoto no projeto de assentamento Santa Júlia, sudoeste do estado do Pará. *Revista Meio Ambiente e Sustentabilidade*, v. 9 (19). <https://doi.org/10.22292/mas.v9i19.895>.
- Vallejo-Villalta, I.; Rodríguez-Navas, E.; Márquez-Pérez, J., 2019. Mapping forest fire risk at a local scale - A case study in Andalusia (Spain). *Environments*, v. 6 (3), 30. <https://doi.org/10.3390/environments6030030>.
- Vettorazzi, C.A.; Ferraz, S.F. B., 1998. Uso de sistemas de informações geográficas aplicados à prevenção e combate a incêndios em fragmentos florestais. *Série Técnica IPEF*, v. 12 (32), 111-115 (Accessed March 12, 2023) at: <https://www.bibliotecaflorestal.ufv.br:80/handle/123456789/14759>.
- Zhang, Z.; Yang, S.; Wang, G.; Wang, W.; Xia, H.; Sun, S.; Guo, F., 2022. Evaluation of geographically weighted logistic model and mixed effect model in forest fire prediction in northeast China. *Frontiers in Forests and Global Change*, v. 5, 1040408. <https://doi.org/10.3389/ffgc.2022.1040408>.